JACS
JOURNAL OF THE AMERICAN CHEMICAL SOCIETY

COMMUNICATION

pubs.acs.org/JACS

Tetrathienoanthracene-Based Copolymers for Efficient Solar Cells

Feng He,[†] Wei Wang,[†] Wei Chen,[‡] Tao Xu,[†] Seth B. Darling,[‡] Joseph Strzalka,[§] Yun Liu,[⊥,¶] and Luping Yu*[,†]

[†]Department of Chemistry and The James Franck Institute, The University of Chicago, 929 E 57th Street, Chicago, Illinois 60637, United States

[‡]Center for Nanoscale Materials, Argonne National Laboratory, 9700 South Cass Avenue, Argonne, Illinois 60439, United States

[§]X-ray Science Division, Advanced Photon Source, Argonne National Laboratory, Argonne, Illinois 60439, United States

[⊥]NIST Center for Neutron Research, National Institute of Standards and Technology, Gaithersburg, Maryland 20899, United States

[¶]Department of Chemical Engineering, University of Delaware, Newark, Delaware 19716, United States

Supporting Information

ABSTRACT: A series of semiconducting copolymers (**PTAT-x**) containing extended π-conjugated tetrathienoanthracene units have been synthesized. It was shown that the extended conjugation system enhanced the $\pi-\pi$ stacking in the polymer/$PC_{61}BM$ blend films and facilitated the charge transport in heterojunction solar cell devices. After structural fine-tuning, the polymer with bulky 2-butyloctyl side chains (**PTAT-3**) exhibited a PCE of 5.6% when it was blended with $PC_{61}BM$.

Scheme 1. Structures of Polymers

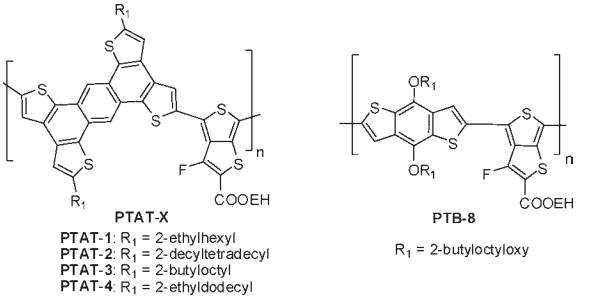

Solar energy, which can be converted into electricity using photovoltaic devices, is the largest renewable energy source. Solar cells based on inorganic semiconductors can harvest solar energy efficiently but with a high cost.[1] Polymeric solar cells (PSCs) based on the bulk heterojunction (BHJ) architecture are thus pursued worldwide due to their distinctive potential for fabrication on flexible substrates with large areas, lightweight, and solution processability at a low cost.[2] By blending electron-donating semiconducting polymers and electron-withdrawing fullerene derivatives together, a bicontinuous interpenetrating network with a large donor−acceptor interfacial area will endow the active layer with large photovoltaic effect.[3] In the past decade, extensive research effort by many groups around the world has revealed promising features of PCSs.[4] Solar energy conversion efficiency larger than 8% has been achieved based on semiconducting polymers developed in this lab.[5]

To explore strategies for further improving solar cell performance and probing structure/property relationships, the effect of dimensionality of conjugated systems on solar cell properties was investigated. The tetrathienoanthracene moiety with two-dimensional (2D) extended π-conjugated structure was chosen as a building block for new polymers,[6] which favors stronger cofacial $\pi-\pi$ stacking. A series of new polymers (**PTAT-x**) were synthesized with thieno[3,4-b]thiophene as comonomer. The results demonstrate that tetrathienoanthracene is a promising building block for the development of semiconducting polymers with high photovoltaic efficiency. Several interesting observations provide insights for further design of photovoltaic polymers.

The structures of the polymers studied here are shown in Scheme 1. The extended π-conjugated system in tetrathienoanthracene will enhance $\pi-\pi$ stacking between the polymer chains; it may also have a side effect of reduced solubility, which will be detrimental to polymer processing. Several monomers with different side chains were thus synthesized in order to obtain processable polymers. At the same time, another **PTB** family polymer, **PTB-8**, with similar bulk side chains as those on **PTAT-3**, with two 2-butyloctyloxy on the benzodithiophene moiety, was also synthesized for the purpose of comparison with **PTAT** polymers.

The synthesis of tetrathienoanthracene monomer is described in the Supporting Information (SI). The bis-trimethyl-stannanyl monomers were polymerized with 2′-ethylhexyl-6-dibromo-3-fluorothieno[3,4-b]thiophene-2-carboxylate by the Stille polycondensation reaction to yield the designed **PTAT** polymers. It was found that polymer **PTAT-1** with 2-ethylhexyl side chains in the tetrathienoanthracene moiety showed poor solubility and were barely processable in organic solvents; this polymer was not investigated further. However, three other new polymers (**PTAT 2−4**) with more bulky side chains are soluble in common organic solvents and exhibit number-average molecular weights (M_n) of 24.1, 18.1, and 18.2 kDa with polydispersity indices (PDI) of 1.6, 2.6 and 2.5, respectively. Since the side chains are bulky and long, **PTB-8** possesses a high M_n of 83.3 kDa with a PDI of 2.05 due to the improved solubility in the polymerization medium.

UV/vis spectra (Figure 1a) of **PTAT2−4** show absorption peaks at 684, 664, and 665 nm with the absorption onset at 747, 737, and 752 nm, which correspond to optical band gaps around

Received: December 9, 2010
Published: February 18, 2011

dx.doi.org/10.1021/ja1110915 | J. Am. Chem. Soc. 2011, 133, 3284–3287

1.66, 1.69, and 1.65 eV, respectively. **PTB-8** showed an absorption peak at 662 nm with an optical band gap at 1.71 eV. It had also been found that the absorption of **PTAT-3** in chloroform is similar to that obtained in films, indicating minimal conformational change from chloroform solution to film. Cyclic voltammograms of **PTAT-3** (SI, Figure S5) showed reversible reduction and oxidation behavior, from which a HOMO energy level of −5.04 eV and a LUMO energy level of −3.28 eV are deduced from the onset potentials, corresponding to a band gap of 1.76 eV, which is quite close to the optical band gap (1.69 eV) of the polymer films. The HOMO and LUMO levels and electrochemical band gaps of other polymers are listed in Table 1. All of these **PTAT** polymers possess low band gaps from 1.76 to 1.80 eV with the HOMO level from −5.04 to −5.12 eV and the LUMO level from −3.28 to −3.32 eV. The band gap of **PTB-8** was found to be slightly increased to 1.90 eV with a HOMO level of −5.24 eV - the lowest among these polymers.

Photovoltaic properties of the polymers were investigated by solar cell structures of ITO/PEDOT:PSS/polymer:$PC_{61}BM$(1:1, w/w)/Ca/Al. The active layers of polymer composites were spin-coated from polymer/$PC_{61}BM$ solutions prepared in chloroform (CF), chlorobenzene (CB), or *o*-dichlorobenzene (DCB), with thickness controlled at around 100 nm. The devices of **PTAT-3** prepared from different solvents exhibited similar open circuit voltage (V_{oc}) at 0.66 V, while there were significant differences in the short circuit current density (J_{sc}) and fill factor (FF). Compared with device from CF/diiodooctane (DIO) solvent, the devices fabricated from CB and DCB showed moderate J_{sc} and relatively low FF: 12.3 mA cm^{-1}, 32% (CB/DIO), and 10.5 mA cm^{-1}, 27% (DCB/DIO) with PCEs about 2.65% (CB/DIO) and 1.91% (DCB/DIO), respectively. When the cosolvent of CF/DIO was used, the J_{sc} of solar cell was significantly enhanced to 15.0 mA cm^{-2}, and a FF of 58% was obtained. The combined effect led to a PCE up to 5.62%. External quantum efficiency (EQE) data from the optimized **PTAT-3**/$PC_{61}BM$ BHJ solar cells are presented in the SI (Figure S6), and the device shows relatively high incident photoconversion efficiency with EQE around 50−60% from 550 to 700 nm.

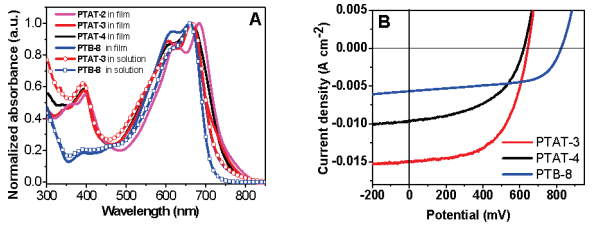

Figure 1. (a) UV/vis absorption spectra of polymers in film and in solution. (b) Current−voltage characteristic of polymer/$PC_{61}BM$ (1:1, w/w) solar cells under AM 1.5 condition (100 mW cm^{-2}).

Solar cells prepared from the other **PTAT-x** polymers were further studied, and representative characteristics are summarized in Table 1. The **PTAT-3** system showed the highest PCE among these polymers. For the 2-ethyldedocyl-substituted polymer, **PTAT-4**, the solubility was found to be poorer than that of **PTAT-3**, leading to a lower J_{sc} (9.6 mA cm^{-1}), FF (50%), and a PCE value of only 2.98%. Another tetrathienoanthracene-based polymer, **PTAT-2**, with the most bulky side chain, showed excellent solubility even in CB and DCB. The devices from CB solution exhibited relatively high V_{oc} of 0.77 V, but low J_{sc} of 1.0 mA cm^{-2}, resulting in a PCE of 0.37%. The low PCE can be attributed to the steric effect of highly bulky 2-decyltetradecyl side chains that will impede the cofacial $\pi-\pi$ stacking in the polymer film. All of these results indicate that the 2-butyloctyl group is the best side chain of those studied for tetrathienoanthracene-based polymers to achieve the optimized solubility and compatibility with fullerene derivatives.

In order to explore the unique features of **PTAT-x** polymers with extended π-system, devices were fabricated using **PTB-8** with similar bulky side chains. Figure 1b showed the $J-V$ curves of the solar cells based on **PTB-8** and **PTAT3−4**. When CF/DIO was used as cosolvent, corresponding devices of **PTB-8**/$PC_{61}BM$ showed a PCE of 2.17% with a V_{oc} of 0.79 V, J_{sc} of 5.1 mA cm^{-2}, and FF of 54%. **PTB-8** exhibits better solar cell

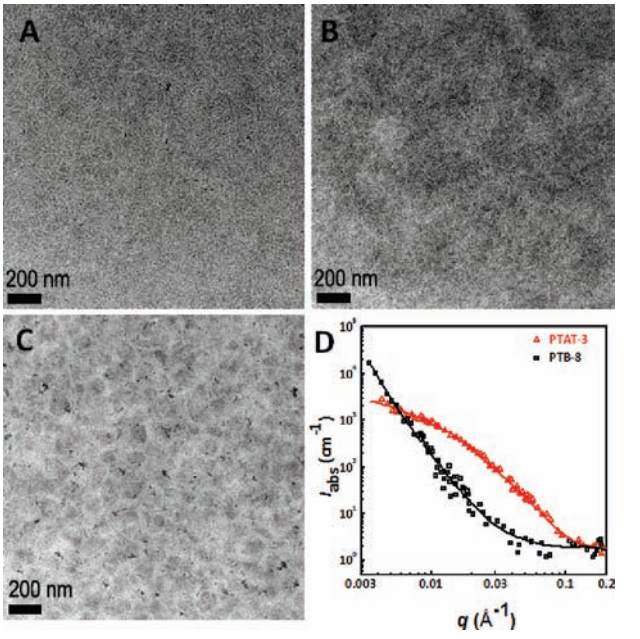

Figure 2. TEM images of polymer/$PC_{61}BM$ blend films. (a) **PTAT-3**/$PC_{61}BM$ from CF/DIO (98/2, v/v); (b) **PTAT-4**/$PC_{61}BM$ from CF/DIO (98/2, v/v); (c) **PTB-8**/$PC_{61}BM$ from CB/DIO (98/2, v/v), the scale bar is 200 nm. (d) SANS profiles for as-spun thin films of **PTAT-3**/$PC_{61}BM$ and **PTB-8**/$PC_{61}BM$.

Table 1. Characteristic Properties of Polymer Solar Cells

polymer	V_{oc} (V)	J_{sc} (mA/cm^2)	FF (%)	PCE (%)	HOMO (eV)	LUMO (eV)	E_g (eV)
PTAT-2[a]	0.77	1.0	0.46	0.37	−5.12	−3.32	1.80
PTAT-3	0.66	15.0	0.58	5.62	−5.04	−3.28	1.76
PTAT-4	0.62	9.6	0.50	2.98	−5.08	−3.31	1.77
PTB-8[a]	0.83	5.7	0.59	2.78	−5.24	−3.34	1.90

[a] Chlorobenzene/DIO (98/2, v/v), 800 rpm; others: chloroform/DIO (98/2, v/v), 2500 rpm.

dx.doi.org/10.1021/ja1110915 |*J. Am. Chem. Soc.* 2011, 133, 3284–3287

properties with a PCE of 2.79% (V_{oc} = 0.83 V, J_{sc} = 5.7 mA cm^{-2}, and FF = 59%) when using CB/DIO as cosolvent, which was still only half of what we achieved with **PTAT-3**.

These results showed that solar cell properties strongly depend on the electronic and solid-state structures. The significant differences among the **PTAT-x** and **PTB-8** are related not only to electronic but also to morphological differences. The purported ideal morphology is comprised of an interpenetrating nanoscale network between donor and acceptor, which enables a large interface area for exciton dissociation and continuous percolating paths for hole and electron transport to the corresponding electrodes. TEM images of **PTAT-3** and **PTAT-4** (Figure 2a,b) with different alkyl chains exhibited fine domains, and no large phases can be found. In contrast, the film of **PTB-8** from CB/DIO shows obvious domains of aggregation as shown in Figure 2c, which suggests that benzodithiophene with 2-butyloctyoxy side chains would reduce the miscibility of **PTB-8** with $PC_{61}BM$ and lead to the low PCE of solar cells via exciton losses.

Since TEM studies generally do not provide definitive information on the 3D phase separation in bulk samples, small angle neutron scattering (SANS) measurements were carried out on **PTAT-3** and **PTB-8**. The SANS profiles for as-spun thin films of **PTAT-3**/$PC_{61}BM$ and **PTB-8**/$PC_{61}BM$ blend films at room temperature are shown in Figure 2d. Using the empirical unified exponential/power-law method developed by G. Beaucage,[7] the averaged domain sizes in **PTAT-3**/$PC_{61}BM$ and **PTB-8**/$PC_{61}BM$ blend films could be achieved as 29 ± 5 and 168 ± 119 nm, respectively. These scattering results are echoed with the TEM data as shown above. It is known that large domains in BHJ solar cells are detrimental to exciton migration and charge separation. The relatively small domain size in the **PTAT-3**/$PC_{61}BM$ film will enhance the donor−acceptor interfacial area and enhance the solar cell properties.

Besides the miscibility with $PC_{61}BM$, the dimensionality of the comonomer will also influence the molecular packing structures significantly. As shown in Figure 3a,b, grazing incidence wide-angle X-ray scattering (GIWAXS) studies revealed that the π-stacking of both **PTAT-3**/$PC_{61}BM$ and **PTB-8**/$PC_{61}BM$ films are parallel to the substrate surface, namely in a face-down orientation that is helpful to hole transport in the polymer films between two electrodes. As shown in Figure 3d, the in-plane linecuts of GIWAXS reveal a lamellar spacing of about 23.7 Å for the **PTAT-3**/$PC_{61}BM$ blend film and 20.4 Å for the **PTB-8**/$PC_{61}BM$ blend film.[8] The difference of about 3.3 Å in polymer lamella distance between **PTAT-3** and **PTB-8** is consistent with the size difference in the comonomer because of the different connection positions of the side chains. The out-of-plane GIWAXS profiles (Figure 3c) show the $\pi-\pi$ distance between the backbones is 3.6 Å for the **PTAT-3**/$PC_{61}BM$ film and 4.1 Å for the **PTB-8**/$PC_{61}BM$ film. Although the scattering arising from the $\pi-\pi$ stacking of polymer backbones in the **PTB-8**/$PC_{61}BM$ blend film overlaps with one of the Bragg diffractions of $PC_{61}BM$, a broadened shoulder showed up around 1.5−1.55 Å^{-1}, which corresponds to the $\pi-\pi$ distance between the backbones. This was further confirmed by GIWAXS results of the neat **PTB-8** homopolymer film (SI, Figure S7). A distinctive scattering was observed in vertical (q_z) of 1.50 Å^{-1}, which coincides with the blend film with a $\pi-\pi$ stacking distance of about 4.1 Å. Therefore, by using extended π-conjugated monomer in **PTAT-3**, the $\pi-\pi$ stacking distance is reduced by 0.5 Å compared to the **PTB-8** polymer with relatively smaller

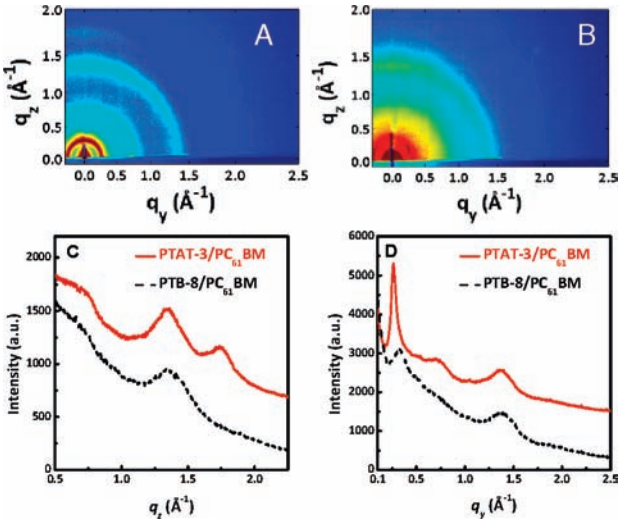

Figure 3. Two-dimensional GIWAXS patterns of the blend films of **PTAT-3**/$PC_{61}BM$ (1:1, w/w) (a) and **PTB-8**/$PC_{61}BM$ (1:1, w/w) (b). (c) Out-of-plane linecuts of GIWAXS of **PTAT-3**/$PC_{61}BM$ and **PTB-8**/$PC_{61}BM$ films. (d) In-plane linecuts of GIWAXS of **PTAT-3**/$PC_{61}BM$ and **PTB-8**/$PC_{61}BM$ films. Note: GIWAXS profiles have been shifted vertically for clarity.

benzodithiophene monomer, which is one of the major reasons why the PCE of devices based on **PTAT-3** is much higher than that of **PTB-8**. This difference is also reflected in the hole mobility, which has been measured by the method based on the space charge limited current (SCLC) model.[9] The hole mobility is found to be around 1.69 × 10^{-4} cm^2 V^{-1} s^{-1} for **PTAT-3** and 1.11 × 10^{-5} cm^2 V^{-1} s^{-1} for **PTB-8**, respectively, which coincides with the GIWAXS results. Higher hole mobility will favor the charge transport in the film devices and, hence, result in better performance.

In conclusion, a series of new semiconducting polymers with extended π-conjugated unit, tetrathienoanthracene, were synthesized. The polymer **PTAT-3** with 2-butyloctyl alkyl side chains exhibited power conversion efficiency about 5.6% with $PC_{61}BM$ from CF/DIO cosolvent. The tetrathienoanthracene can reinforce $\pi-\pi$ stacking in the solid films, which enhanced the device properties through more efficient charge transport. The results indicate that with similar side chains, polymers with larger π systems exhibit better solar cell properties in the systems studied here. However, as the dimensionality of π systems in monomers increases, the poor solubility of the resulting polymers will compromise this advantage. A good solution is to balance the two conflicting effects in search of further enhancement of solar cell properties.

■ ASSOCIATED CONTENT

Supporting Information. Experimental procedures, synthesis of monomers and polymers, cyclic voltammograms, EQE data, and GIWAXS of homopolymer films. This material is available free of charge via the Internet at http://pubs.acs.org.

■ AUTHOR INFORMATION

Corresponding Author
Lupingyu@uchicago.edu

■ ACKNOWLEDGMENT

We acknowledge financial support from NSF, AFOSR, NSF-MRSEC (The University of Chicago). The works described here were also partially supported by Solarmer Energy Inc. Use of the Advanced Photon Source at Argonne National Laboratory and the Center for Nanoscale Materials was supported by the U.S. Department of Energy, Office of Science, Office of Basic Energy Sciences, under Contract No. DE-AC02-06CH11357.

■ REFERENCES

(1) Braga, A. F. B.; Moreira, S. P.; Zampieri, P. R.; Bacchin, J. M. G.; Mei, P. R. *Sol. Energy Mater. Sol. Cells* **2008**, *92*, 418.

(2) (a) Yu, G.; Gao, J.; Hummelen, J. C.; Wudl, F.; Heeger, A. J. *Science* **1995**, *270*, 1789. (b) Brabec, C. J.; Sariciftci, N. S.; Hummelen, J. C. *Adv. Funct. Mater.* **2001**, *11*, 15. (c) Shaheen, S. E.; Brabec, C. J.; Sariciftci, N. S.; Padinger, F.; Fromherz, T.; Hummelen, J. C. *Appl. Phys. Lett.* **2001**, *78*, 841. (d) Li, G.; Shrotriya, V.; Huang, J. S.; Yao, Y.; Moriarty, T.; Emery, K.; Yang, Y. *Nat. Mater.* **2005**, *4*, 864. (e) Thompson, B. C.; Frechet, J. M. J. *Angew. Chem., Int. Ed.* **2008**, *47*, 58.

(3) Yu, G.; Heeger, A. J. *J. Appl. Phys.* **1995**, *78*, 4510.

(4) (a) Wang, E. G.; Wang, L.; Lan, L. F.; Luo, C.; Zhuang, W. L.; Peng, J. B.; Cao, Y. *Appl. Phys. Lett.* **2008**, *92*, 33307. (b) Peet, J.; Kim, J. Y.; Coates, N. E.; Ma, W. L.; Moses, D.; Heeger, A. J.; Bazan, G. C. *Nat. Mater.* **2007**, *6*, 497. (c) Muhlbacher, D.; Scharber, M.; Morana, M.; Zhu, Z. G.; Waller, D.; Gaudiana, R.; Brabec, C. *Adv. Mater.* **2006**, *18*, 2884. (d) Zou, Y. P.; Najari, A.; Berrouard, P.; Beaupre, S.; Aich, B. R.; Tao, Y.; Leclerc, M. *J. Am. Chem. Soc.* **2010**, *132*, 5330. (e) Piliego, C.; Holcombe, T. W.; Douglas, J. D.; Woo, C. H.; Beaujuge, P. M.; Frechet, J. M. J. *J. Am. Chem. Soc.* **2010**, *132*, 7595.

(5) (a) Liang, Y. Y.; Wu, Y.; Feng, D. Q.; Tsai, S. T.; Son, H. J.; Li, G.; Yu, L. P. *J. Am. Chem. Soc.* **2009**, *131*, 56. (b) Liang, Y. Y.; Feng, D. Q.; Wu, Y.; Tsai, S. T.; Li, G.; Ray, C.; Yu, L. P. *J. Am. Chem. Soc.* **2009**, *131*, 7792. (c) Chen, H. Y.; Hou, J. H.; Zhang, S. Q.; Liang, Y. Y.; Yang, G. W.; Yang, Y.; Yu, L. P.; Wu, Y.; Li, G. *Nat. Photonics* **2009**, *3*, 649. (d) Liang, Y. Y.; Xu, Z.; Xia, J. B.; Tsai, S. T.; Wu, Y.; Li, G.; Ray, C.; Yu, L. P. *Adv. Mater.* **2010**, *22*, E135. (e) Liang, Y. Y.; Yu, L. P. *Acc. Chem. Res.* **2010**, *43*, 1227.

(6) Brusso, J. L.; Hirst, O. D.; Dadvand, A.; Ganesan, S.; Cicoira, F.; Robertson, C. M.; Oakley, R. T.; Rosei, F.; Perepichkat, D. F. *Chem. Mater.* **2008**, *20*, 2484.

(7) (a) Beaucage, G. *J. Appl. Crystallogr.* **1995**, *28*, 717–728. (b) Beaucage, G. *J. Appl. Crystallogr.* **1996**, *29*, 134–146.

(8) Guo, J. C.; Liang, Y. Y.; Szarko, J.; Lee, B.; Son, H. J.; Rolczynski, B. S.; Yu, L. P.; Chen, L. X. *J. Phys. Chem. B* **2010**, *114*, 742.

(9) Malliaras, G. G.; Salem, J. R.; Brock, P. J.; Scott, C. *Phys. Rev. B* **1998**, *58*, 13411.